



HAL
open science

Brain network remodelling reflects tau-related pathology prior to memory deficits in Thy-Tau22 mice

Laetitia Degiorgis, Meltem Karatas, Marion Sourty, Emilie Faivre, Julien Lamy, Vincent Noblet, Thomas Bienert, Marco Reisert, Dominik von Elverfeldt, Luc Buée, et al.

► To cite this version:

Laetitia Degiorgis, Meltem Karatas, Marion Sourty, Emilie Faivre, Julien Lamy, et al.. Brain network remodelling reflects tau-related pathology prior to memory deficits in Thy-Tau22 mice. *Brain - A Journal of Neurology* , 2020, 10.1093/brain/awaa312 . hal-03086057

HAL Id: hal-03086057



<https://hal.science/hal-03086057>

Submitted on 17 Nov 2021

HAL is a multi-disciplinary open access archive for the deposit and dissemination of scientific research documents, whether they are published or not. The documents may come from teaching and research institutions in France or abroad, or from public or private research centers.

L'archive ouverte pluridisciplinaire **HAL**, est destinée au dépôt et à la diffusion de documents scientifiques de niveau recherche, publiés ou non, émanant des établissements d'enseignement et de recherche français ou étrangers, des laboratoires publics ou privés.

Brain network remodelling reflects tau-related pathology prior to memory deficits in Thy-Tau22 mice

 Laetitia Degiorgis,¹  Meltem Karatas,^{1,2,3} Marion Soury,^{1,4} Emilie Faivre,⁵ Julien Lamy,¹ Vincent Noblet,¹ Thomas Bienert,² Marco Reisert,² Dominik von Elverfeldt,² Luc Buée,⁵ David Blum,⁵ Anne-Laurence Boutillier,⁶ Jean-Paul Armspach,¹ Frédéric Blanc^{1,7} and Laura-Adela Harsan^{1,8}

In Alzheimer's disease, the tauopathy is known as a major mechanism responsible for the development of cognitive deficits. Early biomarkers of such affectations for diagnosis/stratification are crucial in Alzheimer's disease research, and brain connectome studies increasingly show their potential establishing pathology fingerprints at the network level. In this context, we conducted an *in vivo* multimodal MRI study on young Thy-Tau22 transgenic mice expressing tauopathy, performing resting state functional MRI and structural brain imaging to identify early connectome signatures of the pathology, relating with histological and behavioural investigations. In the prodromal phase of tauopathy, before the emergence of cognitive impairments, Thy-Tau22 mice displayed selective modifications of brain functional connectivity involving three main centres: hippocampus (HIP), amygdala (AMG) and the isocortical areas, notably the somatosensory (SS) cortex. Each of these regions showed differential histopathological profiles. Disrupted ventral HIP-AMG functional pathway and altered dynamic functional connectivity were consistent with high pathological tau deposition and astrogliosis in both hippocampus and amygdala, and significant microglial reactivity in amygdalar nuclei. These patterns were concurrent with widespread functional hyperconnectivity of memory-related circuits of dorsal hippocampus—encompassing dorsal HIP-SS communication—in the absence of significant cortical histopathological markers. These findings suggest the coexistence of two intermingled mechanisms of response at the functional connectome level in the early phases of pathology: a maladaptive and a likely compensatory response. Captured in the connectivity patterns, such first responses to pathology could further be used in translational investigations as a lead towards an early biomarker of tauopathy as well as new targets for future treatments.

- 1 Laboratory of Engineering, Informatics and Imaging (ICube), Integrative multimodal imaging in healthcare (IMIS), UMR 7357, University of Strasbourg, 67000 Strasbourg, France
- 2 Department of Radiology, Medical Physics, University Medical Center Freiburg, Faculty of Medicine, University Freiburg, 79085 Freiburg, Germany
- 3 CNRS, University of Strasbourg, INCI, UMR 7168, 67000 Strasbourg, France
- 4 The University of Sydney, Faculty of Engineering, School of Aerospace, Mechanical and Mechatronic Engineering, NSW 2006 Sydney, Australia
- 5 Univ. Lille, Inserm, CHU Lille, UMR-S 1172 - JPArc, LabEx DISTALZ, F-59000 Lille, France
- 6 Laboratoire de Neurosciences Cognitives et Adaptatives (LNCA), CNRS UMR 7364, 67000 Strasbourg, France
- 7 University Hospital of Strasbourg, CM2R (Memory Resource and Research Centre), Day Hospital, Geriatrics Department, 67000 Strasbourg, France
- 8 Department of Biophysics and Nuclear Medicine, University Hospital of Strasbourg, 67000 Strasbourg, France

Correspondence to: Laura-Adela Harsan

Laboratory of Engineering, Informatics and Imaging (ICube), Integrative multimodal imaging in healthcare (IMIS), UMR 7357, University of Strasbourg, 4 Rue Kirschleger, 67000 Strasbourg, France
E-mail: harsan@unistra.fr

Correspondence may also be addressed to: Laetitia Degiorgis

E-mail: ldegorgis@unistra.fr

Keywords: Alzheimer's disease; resting state connectivity; dementia; functional MRI; tau

Abbreviations: AMG = amygdala; CPu = caudate putamen; DFC = dynamic functional connectivity; d/vHIP = dorsal/ventral hippocampus; rsfMRI = resting state functional MRI; SS(p) = (primary) somatosensory

Introduction

Alzheimer's disease is the most widespread cause of dementia in the world. The belated diagnosis of this pathology, essentially based on clinical features (American Psychiatric Association, 2013) appearing several years after the beginning of the disease (Serrano-Pozo *et al.*, 2011), maintains the important challenge to reveal an early, robust and specific biomarker of Alzheimer's disease.

To date, MRI is the only methodology able to provide a non-invasive insight into the large-scale functional and structural cerebral network architecture, providing the unique possibility to study neurodegenerative diseases at a connectome level (Fornito *et al.*, 2015). Resting state functional MRI (rsfMRI) and diffusion tensor imaging (DTI) are both staple techniques to explore brain functional connectivity modifications in relation to fibre integrity. In Alzheimer's disease patients, functional connectivity modifications of specific networks—including the so called 'default mode network (DMN)'—have been highlighted (Greicius *et al.*, 2004; Sheline and Raichle, 2013), and recent studies show a link between patterns of dynamic functional connectivity (DFC) changes during the rsfMRI scan, and neuropathological affectations (Sourty *et al.*, 2016). Studies using DTI to analyse white matter (Bihan *et al.*, 2001) have supplied evidence of early microstructural changes in Alzheimer's disease mutation carriers (Ringman *et al.*, 2007).

Translation of these approaches into the animal imaging field provides further invaluable opportunities to test and validate these pathophysiological mechanisms by pairing the network analysis with behavioural, genetic, and histological studies. It can reveal the complex interplay between structure and function in the mouse brain and can identify specific therapeutic targets. Such multi-approach strategies in the mouse may provide a unique window to bridge the gap between preclinical and clinical investigations, by direct comparison of whole brain network reconfigurations in response to pathological conditions. In rodents, MRI studies have already highlighted the great potential of this technique as a tool to explore functional and structural connectivity in neurodegenerative models (Harsan *et al.*, 2010; Gozzi and Schwarz, 2015). To evaluate the initial stages of Alzheimer's

disease, studies were conducted on different amyloid mouse models using rsfMRI. They revealed abnormal functional connectivity in several networks, along with alterations in the microstructure of the white matter before cerebral amyloidosis (Grandjean *et al.*, 2014), or associated with toxic soluble amyloid- β (Shah *et al.*, 2016). A recent study (Liu *et al.*, 2018), however, linked local abnormal neuronal activity with the tau pathology in a young mice model of Alzheimer's disease, displaying both amyloid and tau alterations.

Nevertheless, the relationship between alterations of the brain connectome and specific biological substrates of Alzheimer's disease still require a better mechanistic understanding, despite the large and exponentially growing studies in human patients (Liu *et al.*, 2019). Despite the strong implication on the tauopathy in cognitive decline, its impact on circuitry patterns in Alzheimer's disease is still poorly studied. In this context, we performed a non-invasive and *in vivo* brain MRI study of the Thy-Tau22 mouse model progressively expressing brain tauopathy paralleling neuro-immune and cognitive alterations (Schindowski *et al.*, 2006; Van der Jeugd *et al.*, 2013; Laurent *et al.*, 2017). This transgenic model was created by combining G272V and P301S mutations on the 4-repeat isoform of human tau under control of the Thy1.2 promoter. Compared with other transgenic tau models, this mouse model does not present motor deficits, while showing other main Alzheimer's disease-related affectations such as memory impairment (Schindowski *et al.*, 2006; Van der Jeugd *et al.*, 2013; Burlot *et al.*, 2015), disinhibition behaviour, age-dependent pathological tau deposition beginning in the hippocampus (HIP), neurofibrillary tangle (NFT) formation, neuronal death (Belarbi *et al.*, 2009), and gliosis. Based on these studies, the Thy-Tau22 mice model is considered a valuable model to explore and understand the tau pathology. We evaluated possible network signatures at an early pathological stage and identified specific patterns of resting state functional connectivity associated with microstructural alterations. Such circuitry features might underpin early pathological mechanisms in Alzheimer's disease—appearing before behavioural impairment—and constitute new potential biomarkers of prodromal Alzheimer's disease.

Material and methods

Animals

All experimental protocols were approved by the Regional Committee of Ethic in Animals Experiment of Strasbourg (CREMEAS, APAFIS n°2016033011298450). Twelve transgenic Thy-Tau22 and nine littermate wild-type male mice aged 5 months were used for behavioural experiments and MRI studies. We enlarged this cohort for the MRI experiments to improve the statistical analysis by adding four Thy-Tau22 and four wild-type mice of the same age and from the same colony. These animals were not tested for behaviour. Although the expression of the transgene is postnatal in Thy-Tau22 mice, we performed MRI acquisition and analysis in eight transgenic Thy-Tau22 mice and eight wild-types aged 2 months to exclude the possibility of a developmental impact of the transgene expression (Supplementary Fig. 4). All mice were bred on a C57BL6/J background and maintained in a temperature and humidity controlled room under a 12-h light/dark cycle with *ad libitum* access to food and water. Mice were randomly housed in pairs allowing social behaviour. Thy-Tau22 mice overexpressed the human mutated tau protein (G272V and P301S) under the Thy1.2 promoter, inducing formation of phosphorylated tau and, later on, NFTs, throughout the brain (Schindowski *et al.*, 2006).

Behavioural tests

‘Object tasks’ behavioural tests in rodents classically evaluate subtle memory impairments based on animals’ spontaneous behaviour to explore novelty in their environment. We used three types of tests to evaluate the episodic-like memory in mice (Fig. 1A–C): object recognition, object in-place, and object location. These tests were adapted according to previous optimizations (Hamm *et al.*, 2017). Spatial reference learning and memory abilities were evaluated using the Morris Water Maze, as described in Chatterjee *et al.* (2018) (Fig. 1D and Supplementary material).

MRI experiments

Brain MRI was carried out in the two animal groups using a 7 T small bore animal scanner allowing for increased resolutions compared to the routine clinical imaging in human patients, but essential in preclinical environment (BioSpec 70/30, Bruker), a mouse head adapted room temperature surface coil combined with a volume transmission coil, and Paravision 6.0.1 (PV6, Bruker). Anatomical images were acquired using a multislice (34 slices of 0.4 mm) turbo rapid acquisition with relaxation enhancement (RARE) T₂-weighted sequence, as a standard procedure in rodent structural imaging allowing us to keep an adequate acquisition time at high field. RsfMRI data were acquired in 16 min using single shot gradient-echo, echo-planar imaging (GE-EPI). Twenty-seven axial slices of 0.4 mm thickness

were recorded to cover the entire brain (echo time/repetition time = 15/2000 ms, spatial resolution = 0.14 × 0.22 × 0.4). A diffusion tensor imaging – echo planar imaging (DTI-EPI) sequence was used to perform high angular resolution diffusion imaging (HARDI). Twenty-seven slices of 0.5 mm were recorded with 30 diffusion directions and five b-values (500, 1000, 1500, 1750, and 2000 s/mm²), covering the equivalent partition of the brain, as in the rsfMRI scan (Supplementary Table 1). For rsfMRI the animals were briefly anaesthetized with isoflurane for initial animal handling. The anaesthesia was further switched to medetomidine sedation (Domitor[®], Pfizer), initially induced by a subcutaneous bolus injection (0.6 mg medetomidine/kg body weight in 100 µl 0.9% NaCl solution). Fifteen minutes later, the animals received a continuous subcutaneous infusion of medetomidine through an MRI compatible catheter (0.3 mg/kg body weight in 200 µl/h) inserted at the mouse shoulder level. During the whole acquisition, a 2-mm thick agar gel (2% in NaCl) was applied to the mouse head to reduce any susceptibility artefacts arising at the coil/tissue interface. Medetomidine infusion was stopped and replaced by anaesthesia through isoflurane (~1.5% of volume) for further morphological and diffusion-based imaging protocol. Mouse physiological conditions (body temperature and respiration) were monitored continually during the imaging. After the experiment, the animals were allowed to spontaneously recover.

Preprocessing

Preprocessing of functional MRI data was performed using Statistical Parametric Mapping (SPM8, <http://www.fil.ion.ucl.ac.uk/spm/>) with SPMmouse (www.spmmouse.org) for MATLAB (The MathWorks, Natick, Massachusetts) as previously described (Hübner *et al.*, 2017). The SPM function of co-registration was used to realign the first functional scan to its corresponding T₂-weighted image. A step of realignment of the 500 volumes to the first scan was applied as a motion correction (using a least square approach and a six-parameters rigid body transformation in space). Normalization of the T₂-weighted images data was done on a template extracted from the Allen Brain Atlas (<http://mouse.brain-map.org/static/atlas>) involving a linear registration—12-parameter affine transformation—accounting for major differences in head shape and position in-between subjects as well as non-linear registration—warping—accounting for smaller scale anatomical differences. We performed a Gaussian smoothing with a kernel of two voxels full-width at half-maximum (FWHM) to all functional MRI image volumes and a zero-phase band-pass filter was applied to extract frequencies between 0.01–0.1 Hz, representatives of the blood oxygen level-dependent (BOLD) signal. The signal from ventricles was regressed out using a least square approach in order to reduce non-neural detection from the CSF.

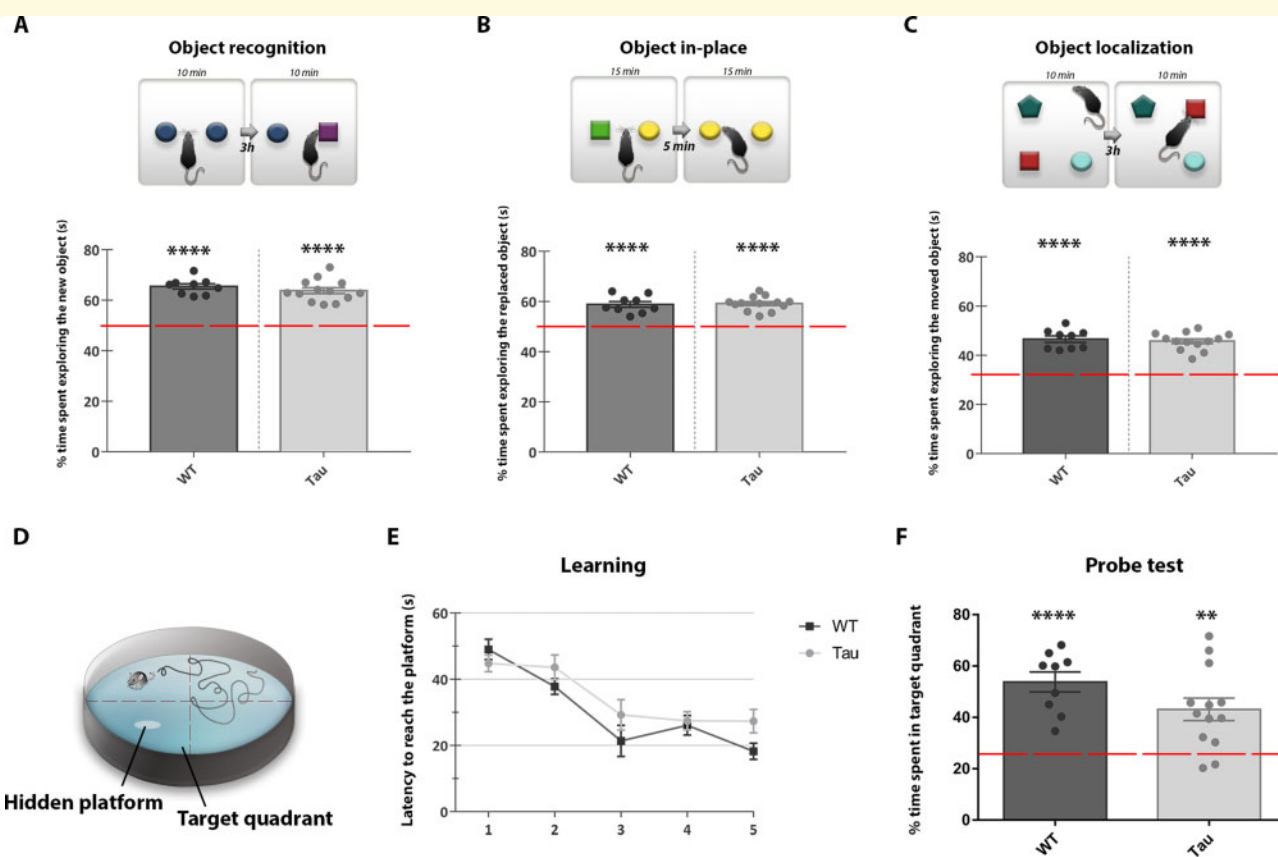


Figure 1 Behavioural evaluation of Thy-Tau22 mice at 5 months. (A) Novel object recognition test, (B) object in-place, and (C) object localization, showing the percentage (%) of time spent exploring the changed object in each test, for both groups [Thy-Tau22 mice and wild-type (WT)] compared with the level of chance (one-sample *t*-test, *****P* < 0.0001; \pm SEM). In the Morris Water Maze test (D) learning abilities (E) were evaluated in each group timing the mean latency to reach the platform over days. Statistical group comparison was performed for each day of training, showing no differences. (F) Probe test performance was evaluated in each group comparing the % of time spent in the target quadrant with the level of chance (25%) (one sample *t*-test, ***P* < 0.01; ****P* < 0.001; *****P* < 0.0001; mean \pm SEM).

Partial correlation analysis

Partial correlation analysis was performed to evaluate direct temporal correlations between spatially separated regions of interest (Smith *et al.*, 2011). Regions of interest ($n = 42$) covering the major mouse brain areas were extracted from the Allen Mouse Brain Atlas (AMBA) (<http://mouse.brain-map.org/static/atlas>), using an in-house built MATLAB tool. Partial correlation coefficients between each pair of regions of interest, by controlling correlation mediated by other regions of interest, were calculated using their associated preprocessed mean time course of the signal. Each element of the matrix represents the strength of functional connectivity between two regions of interest. Partial correlation matrices were generated for each mouse separately and normalized with a Fisher's *z*-transformation. We created: (i) a 42×42 regions of interest matrix covering the major brain areas, to create a ranking of the number of significant connections per region of interest in each group [one sample *t*-test, $P < 0.001$, corrected for multiple comparison; false discovery rate (FDR), as previously described] (Mechling *et al.*, 2014); and (ii) a mean partial correlation matrix for

each group to specifically evaluate functional connectivity of 22 key regions of interest involved in Alzheimer's disease (Fig. 2 and Supplementary Fig. 1). We then created a binary matrix of relevant connections to determine the 'degree' of significant connectivity for each region of interest of the 22×22 matrix, for each group and presented as a graph (Fig. 2A).

Seed-based voxel-wise analysis

Seed-based voxel-wise analysis was performed to evaluate the correlation (Spearman's rho) between the rsfMRI signal's time course of a region of interest, and the time-courses from all other voxels of the brain. We investigated group averaged functional connectivity maps of representative areas showing changed connectivity patterns in partial correlation matrices [i.e. CA1 and primary somatosensory cortex (SSp)]. Group-wise statistical analysis was performed to evaluate functional connectivity modifications of several brain areas, including the dorsal (dHIP) and ventral hippocampus (vHIP) networks. These two regions of interest were

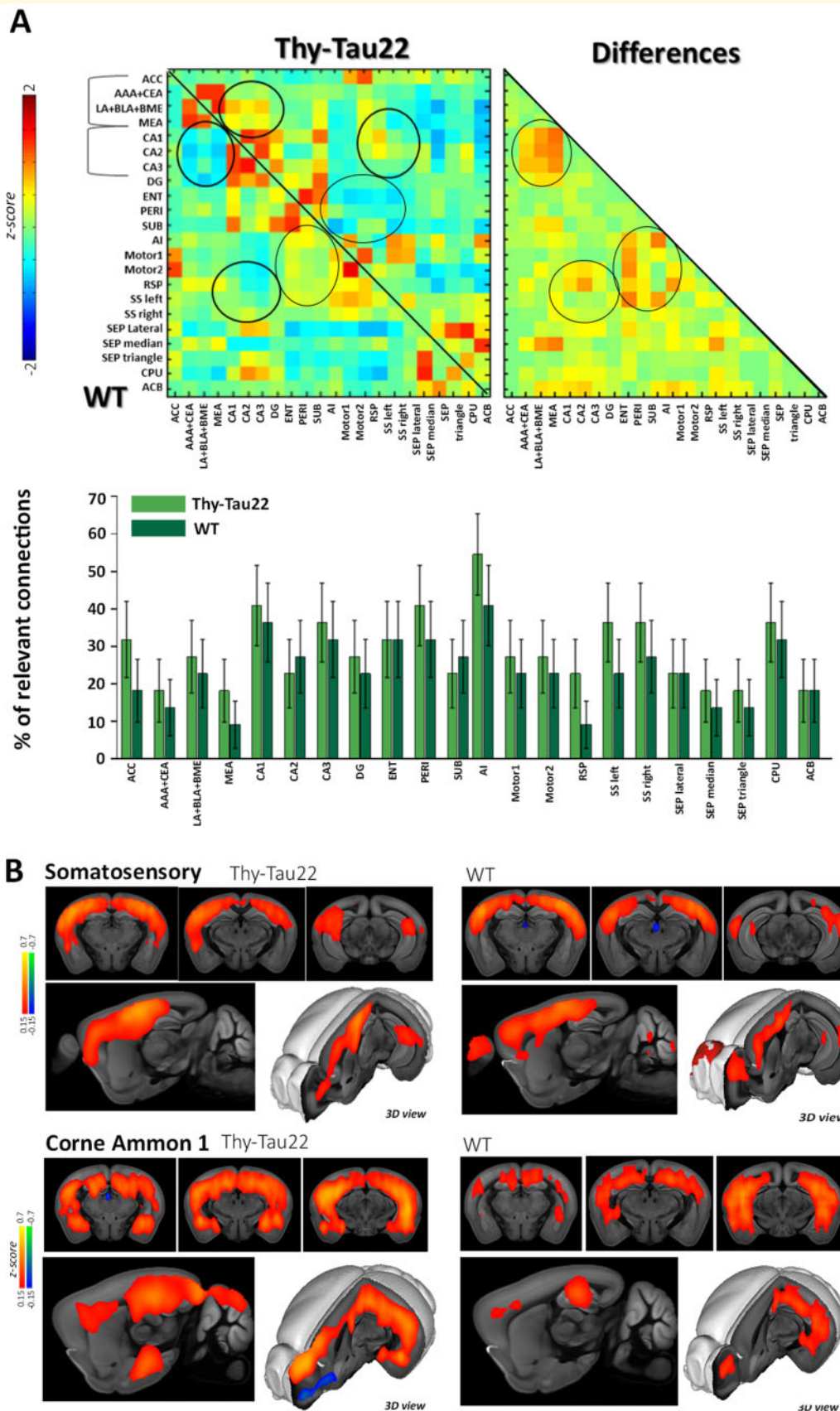


Figure 2 Mean correlation analysis of regions of interest involved in Alzheimer's disease. (A) Mean correlations matrices of BOLD functional connectivity in Thy-Tau22 mice (top) versus wild-type (WT; bottom) on the left, showing functional correlations between pairs of regions of interest. Right: The matrix shows the mean differences in functional connectivity strength in Thy-Tau22 mice versus wild-type. Bottom:

(continued)

created based on parcellation of the whole HIP area extracted from AMBA.

Dynamic functional connectivity

DFC analysis was performed on preprocessed mean time courses extracted from eight regions of interest selected on the basis of their known involvement in Alzheimer's disease and our histological results: dHIP and vHIP, entorhinal cortex, SSp, orbitofrontal area, lateral septal complex, bed nuclei of the stria terminalis, and amygdalar nuclei (AMG). We used a method described in [Sourty *et al.* \(2016\)](#) to compare and characterize connectivity state changes between region of interest's time courses ([Supplementary material and Supplementary Fig. 2](#)).

Structural analysis

For structural analysis, HARDI data were denoised using the MRtrix software ([Veraart *et al.*, 2016](#)), and parametric maps derived from HARDI were generated for each mouse (fractional anisotropy, radial diffusivity, and axial diffusivity). A global fibre tracking approach was used as previously described ([Reisert and Kiselev, 2011](#); [Harsan *et al.*, 2013](#)), to perform global mouse brain tractography. Fibre density maps were constructed for each mouse from the number of streamlines passing in each voxel.

Immunohistochemistry

To quantitatively assess reactive astrocytes and activated microglia/macrophage processes as well as hyperphosphorylated tau distribution on histological brain slices, we performed immunohistochemistry experiments on brain sections of a separate group of mice. We used antibodies against GFAP (glial fibrillary acidic protein), IBA1 (ionized calcium binding adaptor molecule 1), and phosphorylated tau at Ser202/Thr205 sites (AT8 antibody), respectively. In addition, we used the conformation-dependent antibody MC1 to detect misfolded tau protein in Thy-Tau22 mice (a detailed procedure is provided in the [Supplementary material](#)). Quantification analyses of histological staining were performed using ImageJ software, evaluating the percentage of area marked in the HIP, the AMG, and the SS cortex. These areas were selected for quantification based on their consistent connectivity changes detected in rsfMRI. Additionally, we quantified the GFAP and IBA1 intensities in the caudate putamen (CPu), taken as an internal control i.e. devoided of significant group changes in connectivity analysis of the rsfMRI data.

Statistical analysis

To determine performance in objects tasks, we measured the time spent by mice exploring each object for each test. Based on the spontaneous behaviour of rodents to preferentially explore novelty, we expected mice to spend significantly more time exploring the changed, moved or replaced objects. We used a two-way one-sample *t*-test ($P < 0.05$) to compare the percentage of exploration time of each object with the level of chance corresponding to: 50% time for tests involving two objects, and 33% time for the object location tests using three objects. To analyse and compare learning abilities of mice in the Morris Water Maze, we used a one-way ANOVA ($P < 0.05$) with repeated measures, and corrected for multiple comparison by a Tukey test. For the probe test, the time spent in the target quadrant was compared with the chance level (corresponding to 15 s for a test duration of 60 s in four quadrants) using a two-way one-sample *t*-test, $P < 0.01$.

Partial correlation matrices of functional connectivity between regions of interest were generated for each mouse separately and normalized with a Fisher's *z*-transformation. To create a ranking of the number of significant connections per region of interest in each group, we assessed the significance of positive correlations with two-way one-sample *t*-tests thresholded at $P < 0.001$ and corrected for multiple comparison (FDR). To statistically compare functional seed-based networks between groups, we generated Fisher-transformed spatial correlation maps and used a two-way two-sample *t*-test ($P < 0.05$), and applied a cluster-based threshold at $P < 0.05$, corrected for multiple comparisons (FDR) from FSL software. Differences between groups and DFC regions of interest were evaluated using two-way two-sample *t*-test ($P < 0.05$) analysis.

To evaluate structural connectivity modifications between groups, we performed a voxel-based quantification for each type of HARDI-derived map, followed by a two-way two-sample *t*-test to infer microstructural alterations ($P < 0.01$, FDR cluster corrected).

Histological quantification results are expressed as means percentage of the area marked \pm standard error of the mean (SEM) for each region of interest and each staining. Significant differences were determined using one-way ANOVA corrected for multiple comparison (Tukey's test) using Graphpad Prism Software, * $P < 0.05$; ** $P < 0.01$; *** $P < 0.001$; **** $P < 0.0001$.

Data availability

The data that support the findings of this study are available from the corresponding author, upon reasonable request.

Figure 2 Continued

The graph indicates the mean percentage of statistically relevant connections ($P < 0.01$, FDR corrected) for each region of interest of the matrix and each group. **(B)** Coronal slices and 3D representations of the seed-based analysis of CA1 and SSp networks showing the mean correlation between the mean BOLD signal in a region of interest and all other voxels of the brain, in Thy-Tau22 and wild-type mice. The colour scale represents the strength of the functional correlation normalized with a Fisher *z*-transformation. Abbreviations are listed in [Supplementary Fig. 1](#).

Results

Five-month-old Thy-Tau22 mice exhibit preserved memory abilities

To assess the cognitive state of 5-month-old Thy-Tau22 mice, we first performed object memory tests, as sensitive tests to detect potential mild memory alterations in mice. In all tasks, Thy-Tau22 mice did not show any deficit relative to wild-type mice, spending significantly more time exploring the rearranged object during the retention than would be expected from chance ($P < 0.0001$ for each test) (Fig. 1A–C). Mice were then submitted to the Morris Water Maze (Fig. 1D). During the learning phase, both Thy-Tau22 and wild-type mice displayed significant acquisition of the platform location (Day 1 versus Day 5: $P < 0.01$ for Thy-Tau22 and $P < 0.0001$ for wild-type) (Fig. 1E). Analysis of long-term retention (10-day probe test) showed that both groups were able to remember the location of the hidden platform, as they spent significantly more than 25% of the time in the target quadrant (Fig. 1F; $P < 0.01$). There was no genotype effect ($P = 0.42$). Therefore, these data show that different types of memory—relying on different brain structure interactions—are preserved in Thy-Tau22 mice at this age.

Resting state functional MRI modifications in Thy-Tau22 before memory deficits

The analysis of the mean partial correlation connectivity matrix of 22 key regions of interest (Supplementary Fig. 1A), showed increased functional connectivity of hippocampal subregions (CA1, CA3, dentate gyrus) in Thy-Tau22 mice towards cortical areas such as SSp (right and left), retrosplenial cortices as well as most amygdalar nuclei [anterior, central, lateral, basolateral, basomedian and medial AMG) (Fig. 2A). In addition, most regions of interest presented a higher degree of relevant connections in Thy-Tau22 mice than in wild-type (Fig. 2A), denoting a general trend of hyperconnectivity in the Thy-Tau22 mice. The mean correlation maps of the CA1 network (Fig. 2B) suggested a hyperconnectivity of this area especially directed towards SSp cortex, AMG and other HIP subregions (CA2, CA3 and the dentate gyrus). Similarly, the mean correlation maps of AMG (data not shown) and SSp networks (Fig. 2B), indicated increased connectivity patterns of these areas towards HIP. Analysis of the whole brain partial correlation matrix (42×42 regions of interest) suggested a global increase of the functional connectivity in the Thy-Tau22 mice, as the mean number of significant functional connections per regions of interest in Thy-Tau22 was higher (14.5) than in wild-type (11.47), as well as the number of regions displaying a significant number of connections (Supplementary Fig. 1B, $P < 0.001$). Moreover, the ranking of the most connected regions is changed in the transgenic group, particularly highlighting an increase of the connectivity of CA1, SSp,

cortical AMG, perirhinal cortex, orbitofrontal area, anterior cingulate area, and CPU, all above the mean number of connections per region of interest (Supplementary Fig. 1A and B).

To investigate the pattern of these hippocampal functional modifications, we analysed dorsal and ventral hippocampal networks separately.

RsfMRI mapping of dHIP showed a strongly increased mean functional connectivity of this network in Thy-Tau22 compared to wild-type mice (Fig. 3A) towards isocortical regions, within HIP and towards AMG (lateral, basolateral, basomedian). In-between groups statistical comparison showed specific hyperconnectivity of the dHIP in Thy-Tau22 with cortical areas (Fig. 3B), such as a significant bilateral increase of the dHIP-SSp connectivity, and higher correlations with primary motor cortex. The dHIP was also more strongly connected to associative areas like temporal associative and posterior parietal associative areas in Thy-Tau22 than in wild-type as well as perirhinal cortex and entorhinal cortices. Functional connectivity of the dHIP with CPU was found to be stronger in transgenic than wild-type mice.

Statistical analysis of vHIP network (Fig. 4A and B) showed functional modifications in the olfactory system of transgenic mice with decreased functional connectivity strength towards the olfactory bulb, and increased towards piriform and orbitofrontal area cortices. Similar to the dHIP, a significant increase of vHIP-striatum connectivity was found. Interestingly, and opposed to dHIP functional connectivity patterns, vHIP decreased its functional connectivity with AMG in Thy-Tau22 mice, suggesting that HIP subregions communications (dHIP, vHIP) are differently affected in this limbic brain area.

We then evaluated DFC features within eight chosen regions of interest. Results showed that the DFC within those regions of interest was significantly different between groups (two-sample *t*-test, $P < 0.001$). Specific changes of the dynamic features occurred in vHIP DFC and AMG DFC ($P < 0.001$ and $P < 0.0013$, respectively, Supplementary Fig. 2). We further analysed these two regions of interest focusing on only four cognitive states, described in Supplementary Fig. 2. The time spent in three of these four states was significantly different between groups for both regions of interest. Wild-type reached more uncorrelated states than the tau animals who tended to stay in states where more regions of interest are correlated (Supplementary Fig. 2).

To certify that functional modifications detected in 5-month-old mice are not the consequence of a developmental expression of the transgene, we pursued analysis of the mean partial correlation connectivity of 22 key regions of interest in a group of younger (2-month-old) mice (Supplementary Fig. 4A). We found limited increase of functional communication involving intra hippocampal communication, the dentate gyrus (DG) towards CA1, CA2 and DG-AMG; denoting a pattern of hyperconnectivity far more restricted than in 5-month-old mice. Those same regions also displayed early pathological tau deposition, as shown in

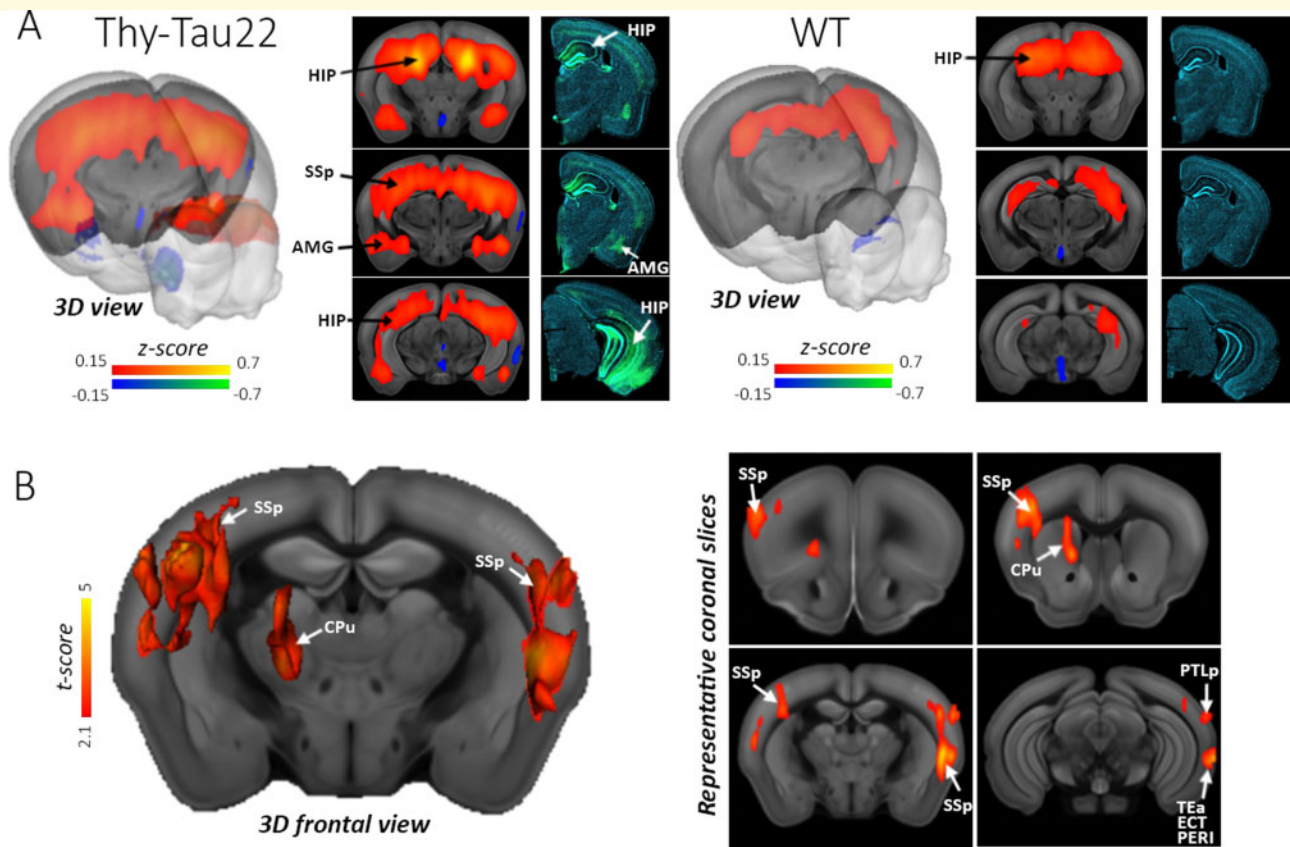


Figure 3 Hyperconnectivity of the dHIP in Thy-Tau22 mice. **(A)** Coronal slices of the seed-based analysis of the dHIP network showing the mean correlation between the mean BOLD signal in the dHIP and all other voxels of the brain, in Thy-Tau22 and wild-type (WT) mice. The colour scale represents the strength of the functional correlation normalized with a Fisher z-transformation. Corresponding coronal slices of immunofluorescence staining are shown to the right of each coronal slice of the seed-based analysis in Thy-Tau22 and wild-type mice: AT8 staining (green) and DAPI (blue). **(B)** Statistical analysis map of the group comparison of dHIP functional connectivity; a significantly higher functional connectivity in Thy-Tau22 mice compared to wild-type is shown in red. 3D representations of statistically significant differences (two sample *t*-test, $P < 0.01$, FDR cluster corrected) is shown on the left. ECT = ectorhinal; PERI = perirhinal cortex; PTLp = posterior parietal associative; TEa = temporal associative.

3-month-old Thy-Tau22 mice sagittal slices with pSer422 staining (Supplementary Fig. 4B).

Microstructural alterations in 5-month-old Thy-Tau22 mice

The group-wise analysis of fractional anisotropy maps showed a significant decrease ($P < 0.01$, FDR cluster corrected) in fractional anisotropy in Thy-Tau22 (Fig. 5A) located bilaterally in the fornix and fimbria, in the internal capsule, and in the CPu. In coherence with these findings, the group-wise fibre density maps statistical comparison showed a decreased fibre density in transgenic mice in the fornix and fimbria, the HIP, lateral septal complex, CPu, the internal capsule and in the thalamus (both medial and ventral part) ($P < 0.01$, FDR cluster corrected; Fig. 5B). No statistically significant changes were detected in radial diffusivity or axial diffusivity. The estimation of volumetric brain changes in Thy-Tau22 mice using voxel-based morphometry

(Supplementary material) analysis showed no differences between groups (data not shown).

Thy-Tau22 brain tissue histology correlates of magnetic resonance-based connectivity modifications

To investigate the pathological microstructural substrate in Thy-Tau22 mice and mechanistically explore the connectivity changes detected with rsfMRI, we performed GFAP, IBA1, AT8 and MC1 immunostaining, and quantitatively evaluated the percentage area of marked cells in AMG, HIP, and SS cortex; and in CPu for GFAP and IBA1 (Fig. 6). GFAP staining revealed significant astrogliosis features in dHIP, vHIP, and AMG in Thy-Tau22 mice ($P < 0.0001$), but not statistically significant astrogliotic reactions in the SS and CPu areas when compared to wild-type mice (Fig. 6B). We additionally quantified the microglial response with IBA1 and detected a specific tendency ($P = 0.052$) of

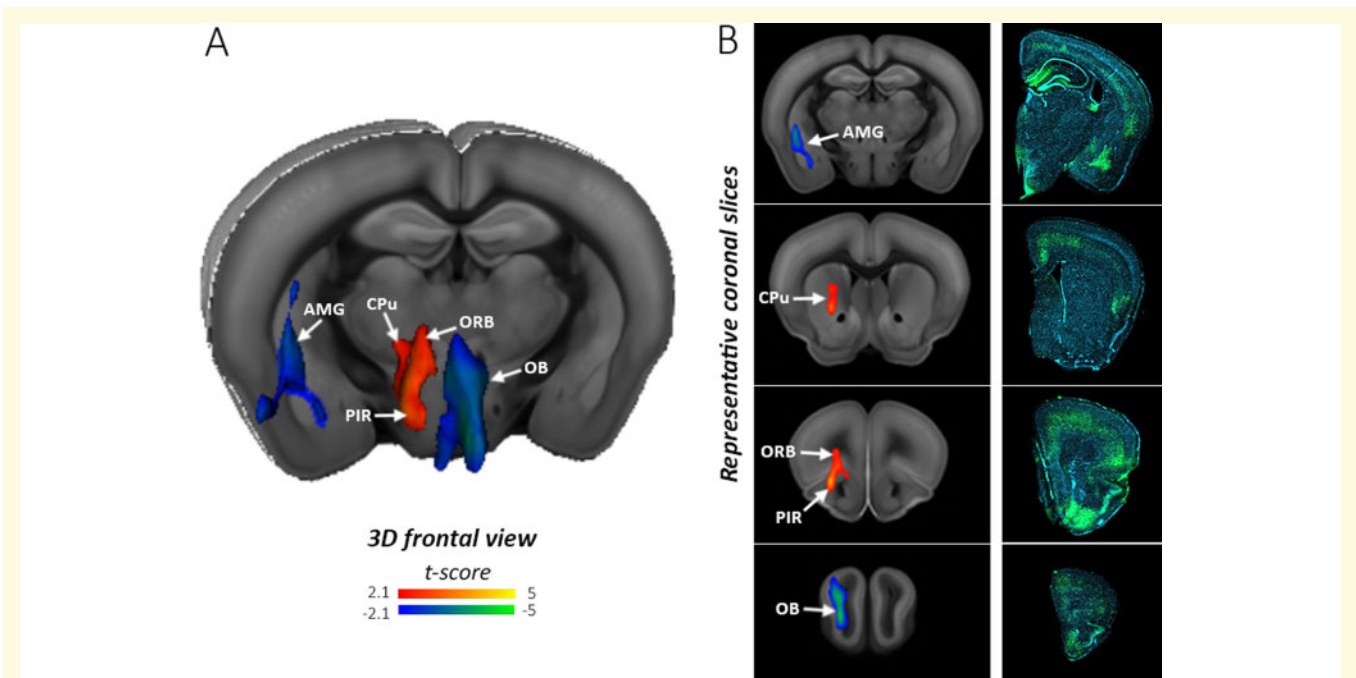


Figure 4 Functional modifications of the vHIP in Thy-Tau22 mice. (A) 3D representation of the group comparison statistical results of vHIP functional connectivity; significantly higher functional connectivity is shown in red and a significantly lower functional connectivity is shown in blue, in Thy-Tau22 mice than in wild-type (WT) (two-sample t -test, $P < 0.01$, FDR cluster corrected). (B) Coronal slices of the functional connectivity statistical map and corresponding slices of immunofluorescence staining in a Thy-Tau22 mouse: AT8 staining (green) and DAPI (blue); in the middle and on the right, respectively. OB = olfactory bulb; ORB = orbitofrontal area; PIR = piriform.

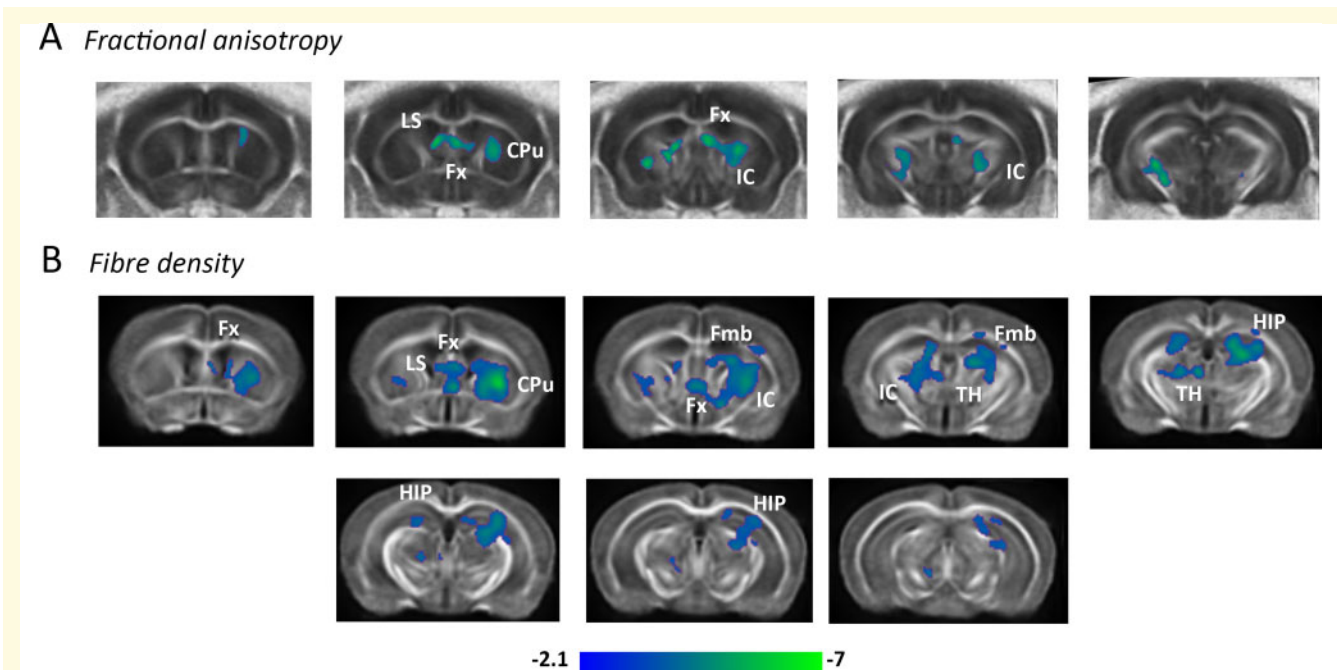


Figure 5 Microstructural modifications at the early stage of tauopathy. Statistical group comparison of fractional anisotropy (A) and fibre density (B) between Thy-Tau22 and wild-type (WT) (two-sample t -test, $P < 0.01$, FDR cluster corrected). Colour scale representing a significant decrease in fractional anisotropy and fibre density in Thy-Tau22 mice. fx = fornix; IC = internal capsule; Fmb = fimbria; TH = thalamus; LS = lateral septal complex.

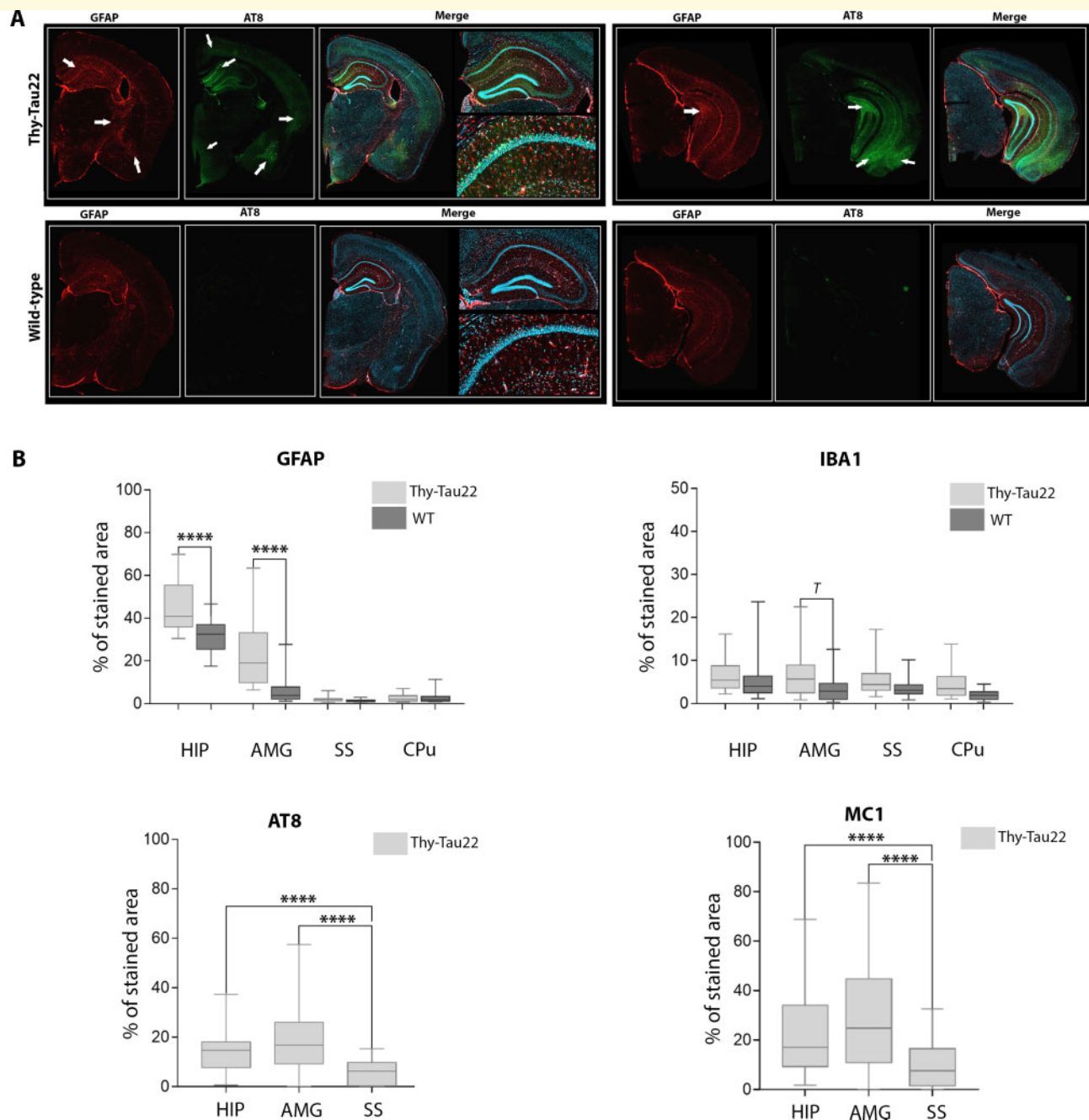


Figure 6 Immunohistological investigation of the inflammatory response and tauopathy in Thy-Tau22 mouse brain. (A) Representative immunofluorescence coronal slices of AT8 (green), GFAP (red), and merged images with DAPI (blue) in Thy-Tau22 and wild-type (WT) mice. Arrows indicate the highest intensity of staining. (B) Quantitative analysis of the immunostainings. GFAP and IBA1 staining (top) in the combined dorsal and ventral hippocampus (HIP), AMG, SS cortex and CPu are shown comparatively in Thy-Tau22 and wild-type mice. Quantification of tauopathy markers is represented below. The stained percentage area of AT8 and MC1 reactivity is measured in HIP, AMG, and SS of Thy-Tau22. Only background noise is detectable in the wild-type histological slices of both stains. Statistical differences were assessed using one-way ANOVA corrected for multiple comparison (Tukey's test, * $P < 0.05$; ** $P < 0.01$; *** $P < 0.001$; **** $P < 0.0001$).

increased IBA1 in AMG of Thy-Tau22 mice—indicating an inflammatory response—but not in the other evaluated regions of interest. Alternatively, AT8 and MC1 staining showed the highest tau deposition in the AMG (referred to

the staining percentage area of phosphorylated and misfolded tau), followed by HIP then the SS cortex ($P < 0.0001$, Fig. 6B) of Thy-Tau22 mice. Several other brain areas showed pathological tau depositions in

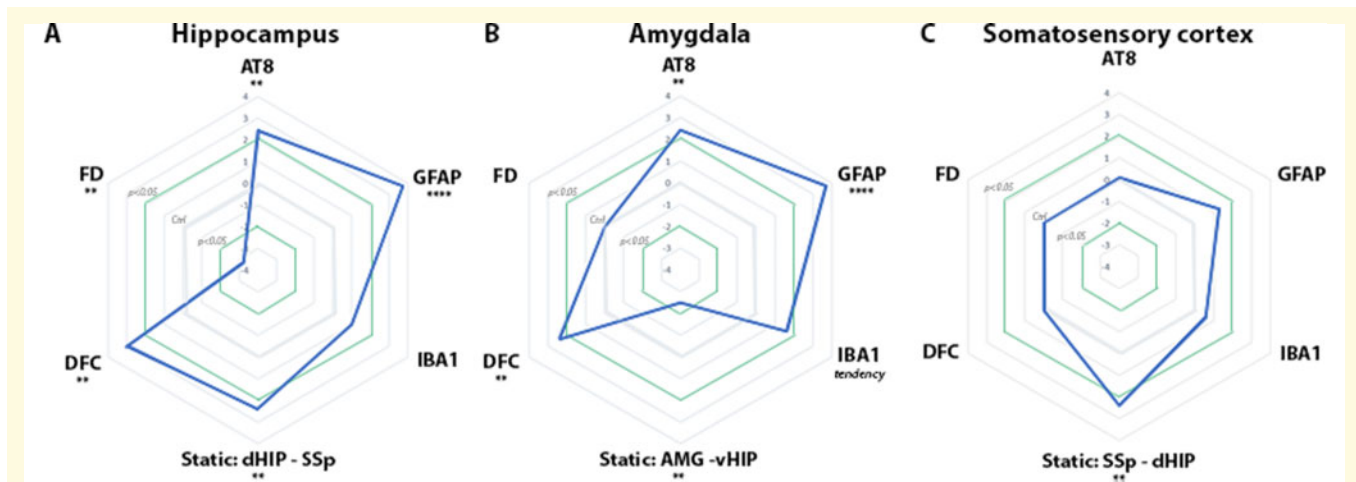


Figure 7 Multivariate representation of the pathological environment in Thy-Tau22. Comparative representation of the pathological modifications in the HIP, AMG and SS cortex, combining imaging and histological changes reaching significance in intergroup comparison. Z-scores of statistical differences between Thy-Tau22 and wild-type mice are represented for each brain area pooling changes in AT8, GFAP and IBA1 staining; fibre density (FD); DFC; and a representative pathway of the static functional communication for each area showing statistically significant connectivity differences between two representative areas extracted from seed analysis. The green lines indicate the $P < 0.05$ thresholds of significance (increase or decrease); relative to the control wild-type parameters (bold grey line). **(A)** The HIP plot indicates a combined significant increase of hyperphosphorylated tau (AT8) deposition and astrogliosis (GFAP); biological features that are reflected as a decrease in the fibre density mapping and translated into the hypersynchrony of the BOLD rsfMRI static connectivity between dHIP and SSp area. The same tendency of hyperconnectivity was highlighted between dHIP and AMG in the seed correlation maps (Fig. 2). This particular pattern of hyperconnectivity might be seen as a functional compensation of the dHIP, as a consequence of the astrocytic response and affected microstructure. **(B)** Multi-parametric characterization of the AMG shows that this brain structure is a central target of tau pathology. Additional to significant AT8 and GFAP increases, IBA1 staining indicates significant reactive microglia processes and therefore an inflammatory response. These findings advocate for a more advanced AMG pathology, leading in this case to a decrease of the AMG-vHIP communication and altered patterns of dynamic connectivity of this region. **(C)** Multivariate representation of metrics related to the SS cortex do not show any significant pathological features of AT8, GFAP and IBA1; fibre density and DFC are also unchanged for this area. The SSp cortex is, however, exhibiting an increased functional connectivity with dHIP in static functional connectivity analysis, which supports the suggested involvement of the SS cortex in a compensatory response due to HIP and AMG affectations.

qualitative microscopy evaluation such as orbitofrontal area, temporal associative, entorhinal, perirhinal, and entorhinal cortices, as illustrated in Fig. 6A. Only background noise was detectable in the wild-type histological slices for these tau pathology markers.

Discussion

This study provides strong evidence regarding the early tauopathy impact on the brain connectivity, demonstrating that dysregulation of neuronal network activity precedes memory and learning deficits. We show specific modifications of the functional brain communication of key memory regions, such as the HIP, AMG and cortical areas, in a tauopathy mouse model of Alzheimer's disease. We equally show for the first time that dynamic features of the functional connectivity between such regions are also perturbed. Moreover, these functional connectivity results were attuned with microstructural alterations along HIP-related pathways (Supplementary Fig. 3).

We tested memory and learning abilities of 5-month-old Thy-Tau22 mice using established approaches, recruiting

key memory areas presenting tauopathy in Alzheimer's disease (Braak et al., 2006): HIP, entorhinal cortex, perirhinal cortex and cortical regions (Lee and Solivan, 2008; Clarke et al., 2010; Van Cauter et al., 2013). In all tests, Thy-Tau22 mice demonstrated good performance, supported by a previous study showing spatial memory impairment starting around 8–9 months, and non-spatial memory impairment starting at around 6 months of age in Thy-Tau22 mice (Van der Jeugd et al., 2013). Despite this lack of an Alzheimer's disease-specific phenotype at 5 months, these mice are developing pathological tau hyperphosphorylation in the HIP as early as 3 months of age, according to the literature. Altogether those results show that the 5-month-old Thy-Tau22 mouse model is reliable for studying early onset of the disease, with neither cognitive impairment, synaptic degeneration (Burlot et al., 2015; Chatterjee et al., 2018) nor neuronal loss.

We quantified global remodelling of the functional connectome in these mice, revealing a hyperconnectivity signature of HIP-cortical and altered HIP-AMG functional communication in Thy-Tau22 brain, but also major modifications of the intra-HIP network, and HIP versus temporal areas, prefrontal cortices.

Interestingly, those same functional paths have been shown to be affected in patients with mild cognitive impairment (MCI) (Stephen *et al.*, 2010). Several groups showed functional hyperconnectivity of the HIP in MCI patients during memory tasks while structural analysis demonstrated atrophy of this same region (Dickerson *et al.*, 2005; Bakker *et al.*, 2012). Moreover, a recent study modelling morphological changes in brain areas across lifespan in Alzheimer's disease patients versus controls revealed an early vulnerability and a close abnormal evolution of the HIP and AMG (Coupé *et al.*, 2019). Other groups showed early modifications of the functional connectivity in the SSp and motor cortices functional circuitry (Grandjean *et al.*, 2014) and hyperconnectivity of the HIP (Shah *et al.*, 2016) before amyloid plaque depositions in mice models of amyloidosis. Using 3-month-old amyloid mice, a study detected hypersynchronous signals in the HIP and frontal networks of mice presenting early impairment in cognitive flexibility but not in classic memory test (Latif-Hernandez *et al.*, 2019). Recently a regional homogeneity study of the BOLD signal in young transgenic mice expressing both amyloid and tau pathologies established a correlation between the hypersynchronous signal in the HIP, parietal, and temporal cortices; and the presence of pathological tau (Liu *et al.*, 2018). Despite the trend to interpret hypersynchrony as a compensatory mechanism that might help the maintenance of a normal behaviour by several authors, other evidence supports the idea that an increased hippocampal functional connectivity could reflect a dysfunctional condition, whose reduction could improve cognition in patients (Bakker *et al.*, 2012).

We further investigated the hippocampal connectivity studying dorsal and ventral HIP functional networks separately (Fanselow and Dong, 2010). We found an increase functional connectivity of the dHIP network towards cortical brain areas—a pathway that has been proved to be indispensable, especially in spatial memory processes (Jones and Wilson, 2005)—in Thy-Tau22 mice. This hyperconnectivity may reflect a compensatory adaptation regarding the strong pathological tau deposition in the dHIP, inducing an increased functional connectivity towards recruited remote brain areas, and allowing the preservation of the behavioural output in Thy-Tau22 mice (Fornito *et al.*, 2015). As suggested by previous studies on primary neuronal cultures (Wu *et al.*, 2016), higher neuronal activity would trigger tau release and propagation. In our study, we did not find significant differences in pathological tau deposition in the SSp between Thy-Tau22 and wild-type mice; even so this area showed a significant increased functional connectivity with the dHIP. Therefore, this higher functional communication does not seem to be responsible for enhancing the tau pathology in our model.

The vHIP is crucially involved in olfactory processes, exhibiting numerous afferences directed to the olfactory bulb and the piriform cortex, before projecting to the orbitofrontal area cortex (Fanselow and Dong, 2010). Major modifications of functional interactions with those regions has been found while investigating the vHIP functional connectivity,

despite that Thy-Tau22 mice only present olfactory impairment from 12 months, as shown by Martel *et al.* (2015). These alterations might illustrate a compensatory increase of the vHIP-piriform and vHIP-orbitofrontal area cortices functional connectivity, counteracting the decrease of its functional communication with the olfactory bulb. In accordance with human studies (Kovács, 2004), we detected a high density of pathological tau in the olfactory bulb in Thy-Tau22 mice. These results reinforce a link between pathological tau depositions and functional connectivity disruptions in Alzheimer's disease. The decrease of the vHIP-olfactory bulb functional connectivity could reflect a threshold level of the phosphorylated tau density that would rather induce functional hypoconnectivity than hyperconnectivity. Supporting evidence of early olfactory dysfunction in pre-symptomatic Alzheimer's disease patients has already been shown (Wilson *et al.*, 2009) and proposed as an early maker of Alzheimer's disease.

Specific connections between the AMG and the vHIP are responsible for the emotional arousal effect on encoding and consolidation of memories (Phelps, 2004). Alzheimer's disease patients display atrophy of the AMG and disruptions in related function relying on the HIP-AMG complex (Poulin *et al.*, 2011; Miller *et al.*, 2015; Coupé *et al.*, 2019). Our investigation of the vHIP functional network showed a decrease of the vHIP-AMG functional connectivity in Thy-Tau22. Supporting these results, analysis of the DFC demonstrated specific modifications in vHIP and in AMG dynamic communication in transgenic mice, which preferentially stayed in highly correlated states. Additionally, a high density of pathological tau deposition, astroglia and microglia markers was found in amygdalar nuclei of Thy-Tau22 mice. Thus, the decrease of the vHIP-AMG functional interaction could be related to microstructural affectations. This pattern of disruption better overlaps with dynamic functional MRI features than with static connectivity metrics, which also display a potential compensatory mechanism involving dHIP and cortical areas. However, differential functional alterations of ventral and dorsal subregions of the hippocampus were detected in both dynamic and static analysis, and most likely arise from complex within-network pathological mechanisms, that were not highlighted with histological quantifications. Evidence of functional alterations of the AMG in MCI patients (Yao *et al.*, 2013; Ortner *et al.*, 2016) are in-line with our findings suggesting a specific alteration of the HIP-AMG pathways of connectivity, leading to differential affectations of dorsal and ventral HIP at early stages of Alzheimer's disease. The astrogliosis found in the same regions also raises the hypothesis of astrocyte involvement in this abnormal signal, as supported previously in a mouse model study of amyloidopathy (Kuchibhotla *et al.*, 2009).

The limited functional hyperconnectivity observed in Thy-Tau22 mice at 2 months of age are spatially linked with the onset of pathological tau deposition in the same areas (HIP and AMG). These findings attest progressive alterations of the functional brain architecture, specifically affecting areas

showing even minimal pathological tau deposition in HIP and AMG. This effect is not due to the Thy1.2 promoter activity during embryonic CNS development as transgene expression can only be detected from postnatal Day 11 (Supplementary Fig. 4C).

Our diffusion MRI investigation of white matter integrity showed alterations of the internal capsule connecting the basal ganglia, the HIP and cortical centres. Linking structural with functional connectivity, it has been shown that minimal structural damage can be sufficient to trigger an increase of functional connectivity towards compensatory mechanisms (Fornito *et al.*, 2015). Therefore, microstructural alterations along this cortico-subcortical pathway may result in failure of the efficient functional reorganization, participating in the functional hyperconnectivity in these regions in Thy-Tau22 mice. A decrease of the fractional anisotropy and fibre density in the fornix, the lateral septum, the fimbria and the HIP, illustrated microstructural modifications of the septo-hippocampal pathway in transgenic mice, a cholinergic tract connecting the HIP with septal nuclei (Thomas *et al.*, 2011). Affections of the fornix-fimbria complex have also been shown in Alzheimer's disease patients (Copenhaver *et al.*, 2006; Thomas *et al.*, 2011), Thy-Tau22 mice (Belarbi *et al.*, 2009) and on the VLW mouse strain expressing tauopathy (Soler *et al.*, 2017), but never at a prodromal stage of the disease.

Tau deposition and astrogliosis were noticed in the septum of Thy-Tau22 on qualitative inspection of the brain sections. This feature might itself contribute to the decrease of fractional anisotropy and fibre density; initiating subtle microstructural affection of projecting tracts from this area, notably along the septo-hippocampal connection. With this, altered fibre density and fractional anisotropy found in CPu and thalamus of transgenic mice provide evidence of structural affections to the whole limbic system architecture (Rajmohan and Mohandas, 2007). Therefore, the alteration of the dorso-ventral structural connectivity of the limbic system may be a crucial mechanism underlying early functional alterations in Alzheimer's disease, suggested by the functional hypersynchrony of the dHIP towards AMG and CPu, and a higher functional connectivity in prefrontal areas. However, we did not have any specific axonal or myelin staining performed in our study to assert and demonstrate a specific structural damage/loss of these two components at such an early age. Fractional anisotropy and/or fibre density changes are usually related to pathological processes leading to loss of tissue (Kochunov *et al.*, 2007), Wallerian degeneration (Xie *et al.*, 2012) and demyelination, but also inflammatory processes (Zhan *et al.*, 2018). We thus suggest that the decrease of these parameters in the white matter and Thy-Tau22 might be related to astrogliosis detected in the HIP, AMG and septal complex affecting the integrity of their connecting system.

We further tested a potential tissue/neuronal loss in the transgenic mice using voxel-based morphometry. We did not detect any morphometric alterations, which indicates that tissue/neuronal loss is not yet occurring at this age in the

Thy-Tau22 group. Schindowski *et al.* (2006) detected a decrease of pyramidal cell numbers in CA1 starting only at 12 months, concurrent with affectations of the synaptic excitability of CA1 associated with both synaptic loss and/or malfunction in the Thy-tau22 model. White matter lesion volume and DTI metrics were also correlated with level of serum neurofilament light chain levels in a longitudinal evaluation in Alzheimer's disease patients (Schultz *et al.*, 2020).

With non-invasive structural and functional MRI, we identify patterns of brain communication that may be pursued as biomarkers of early tau pathology, before the emergence of memory and learning deficits. We show a relationship between these vulnerable circuits and histological markers, stating for the coexistence of two mechanisms of response at connectome level in the early phases of pathology: a maladaptive and a compensatory response, that are intermingled and involving three main centres: HIP, AMG and the isocortical areas, notably the SS cortex. First, from microstructural analysis we detected most of the anisotropy loss and modifications in the mapping of the fibre density in the dHIP and along its connectional system: septo-hippocampal pathway including fornix and fimbria, and striatal and thalamic tracts. The main histological correlates are the significant pathological tau deposition and astrogliotic response in the same area. The microglial reactivity is not a significant player. These biological processes are linked with the hyperconnectivity of the dHIP with both AMG and SS cortex. Of particular interest is the pattern of hyperconnected state with the SS cortex in the absence of statistically significant tau deposition, astrogliotic and microglial response in this cortical area. This finding supports the hypothesis of a compensatory remodelling of dHIP-SS functional pathway, in response to the HIP affectations and the more advanced pathology involving vHIP-AMG communication. Indeed, tau pathology, reactive astrogliosis and the microglial reactivity are statistically relevant in the AMG of Thy-Tau22 when compared with the wild-type mice; but also show a stronger pathological profile when compared to the quantitative analysis of the HIP histological markers in the transgenic group. This is translated into altered dynamic connectivity profiles of AMG and vHIP, and disrupted vHIP-AMG functional pathway in static functional connectivity analysis. Although our quantitative analysis was focused on the HIP, AMG and SS—the network's nodes that were central to our rsfMRI findings—the qualitative analysis of the brain tissue indicates pathological tau deposition in other brain regions, including septal and ventral striatal subcortical areas, orbital, perirhinal, entorhinal and entorhinal cortex cortices, eventually triggering a compensatory mechanisms of functional hyperconnectivity, that we globally assess at this early stage.

These signatures could further be used in translational investigations as a lead towards early diagnosis and prediction, as well as new targets for future treatments. Probing the brain networks in animal models is a key strategy to shed light on mechanisms of the pathology and advance the

translational research. Indeed, showing such early functional hyperconnectivity in a mouse model expressing only tauopathy could help understand results in MCI subjects suggesting that cortical hypermetabolism at early onset of the disease would reflect a compensatory mechanism, particularly in amyloid-negative patients (Ashraf *et al.*, 2015). MRI is today part of this synergistic strategy, as its non-invasive and versatile nature allows for both clinical and preclinical analysis.

In conclusion, our approach synergized information from multivariate imaging and histology, allowing for observation of multifactorial biological processes and enabling future modelling of such factor-factor interactions.

Acknowledgements

The authors wish to thank Pr. Jonathan Brouillette for the molecular experiments to verify the transgene expression, Mary Mondino for her help on data processing, Dr Céline Meillier for very helpful discussions regarding functional image processing, Dr Chantal Mathis for kindly providing supply and guidance for behavioural tests and Dr Chrystelle Po for her technical support at the MRI scanner. The project was developed using the IRIS imaging facility of ICube lab, Strasbourg.

Funding

This work is supported by the Alsace Region for the PhD Fellowship of Laetitia Degiorgis and the Alsace Alzheimer Foundation. L.B.'s laboratory is supported by Programs d'Investissements d'Avenir LabEx (excellence laboratory) DISTALZ (Development of Innovative Strategies for a Transdisciplinary approach to ALZheimer's disease). M.S. is supported by the Australian Research Council grant (DP170101815).

Competing interests

The authors report no competing interests.

Supplementary material

Supplementary material is available at *Brain* online.

References

- American Psychiatric Association. Diagnostic and Statistical Manual ental Disorders (5th edition). American Psychiatric Association; 2013. Available from: <https://psychiatryonline.org/doi/book/10.1176/appi.books.9780890425596>.
- Ashraf A, Fan Z, Brooks DJ, Edison P. Cortical hypermetabolism in MCI subjects: a compensatory mechanism? *Eur J Nucl Med Mol Imaging* 2015; 42: 447–58.
- Bakker A, Krauss GL, Albert MS, Speck CL, Jones LR, Stark CE, et al. Reduction of hippocampal hyperactivity improves cognition in amnesic mild cognitive impairment. *Neuron* 2012; 74: 467–74.
- Belarbi K, Schindowski K, Burnouf S, Caillierez R, Grosjean M-E, Demeyer D, et al. Early Tau pathology involving the septo-hippocampal pathway in a Tau transgenic model: relevance to Alzheimer's disease. *Curr Alzheimer Res* 2009; 6: 152–7.
- Bihan DL, Mangin J-F, Poupon C, Clark CA, Pappata S, Molko N, et al. Diffusion tensor imaging: concepts and applications. *J Magn Reson Imaging* 2001; 13: 534–46.
- Braak H, Alafuzoff I, Arzberger T, Kretschmar H, Del Tredici K. Staging of Alzheimer disease-associated neurofibrillary pathology using paraffin sections and immunocytochemistry. *Acta Neuropathol* 2006; 112: 389–404.
- Burlot M-A, Braudeau J, Michaelsen-Preusse K, Potier B, Ayciriex S, Varin J, et al. Cholesterol 24-hydroxylase defect is implicated in memory impairments associated with Alzheimer-like Tau pathology. *Hum Mol Genet* 2015; 24: 5965–76.
- Chatterjee S, Cassel R, Schneider-Anthony A, Merienne K, Cosquer B, Tzeplaeff L, et al. Reinstating plasticity and memory in a tauopathy mouse model with an acetyltransferase activator. *EMBO Mol Med* 2018; e8587.
- Clarke JR, Cammarota M, Gruart A, Izquierdo I, Delgado-García JM. Plastic modifications induced by object recognition memory processing. *Proc Natl Acad Sci USA* 2010; 107: 2652–7.
- Copenhaver BR, Rabin LA, Saykin AJ, Roth RM, Wishart HA, Flashman LA, et al. The fornix and mammillary bodies in older adults with Alzheimer's disease, mild cognitive impairment, and cognitive complaints: a volumetric MRI study. *Psychiatry Res Neuroimaging* 2006; 147: 93–103.
- Coupé P, Manjón JV, Lanuza E, Catheline G. Lifespan changes of the human brain in Alzheimer's disease. *Sci Rep* 2019; 9: 3998.
- Dickerson BC, Salat DH, Greve DN, Chua EF, Rand-Giovannetti E, Rentz DM, et al. Increased hippocampal activation in mild cognitive impairment compared to normal aging and AD. *Neurology* 2005; 65: 404–11.
- Fanselow MS, Dong H-W. Are the dorsal and ventral hippocampus functionally distinct structures? *Neuron* 2010; 65: 7–19.
- Fornito A, Zalesky A, Breakspear M. The connectomics of brain disorders. *Nat Rev Neurosci* 2015; 16: 159–72.
- Gozzi A, Schwarz AJ. Large-scale functional connectivity networks in the rodent brain. *Neuroimage* 2015; 127: 496–509.
- Grandjean J, Schroeter A, He P, Tanadini M, Keist R, Krstic D, et al. Early alterations in functional connectivity and white matter structure in a transgenic mouse model of cerebral amyloidosis. *J Neurosci* 2014; 34: 13780–9.
- Greicius MD, Srivastava G, Reiss AL, Menon V. Default-mode network activity distinguishes Alzheimer's disease from healthy aging: evidence from functional MRI. *Proc Natl Acad Sci USA* 2004; 101: 4637–42.
- Hamm V, Héraud C, Bott J-B, Herbeaux K, Strittmatter C, Mathis C, et al. Differential contribution of APP metabolites to early cognitive deficits in a TgCRND8 mouse model of Alzheimer's disease. *Sci Adv* 2017; 3: e1601068.
- Harsan L-A, David C, Reisert M, Schnell S, Hennig J, von Elverfeldt D, et al. Mapping remodeling of thalamocortical projections in the living reeler mouse brain by diffusion tractography. *Proc Natl Acad Sci USA* 2013; 110: E1797–E1806.
- Harsan L-A, Paul D, Schnell S, Kreher BW, Hennig J, Staiger JF, et al. In vivo diffusion tensor magnetic resonance imaging and fiber tracking of the mouse brain. *NMR Biomed* 2010; 23: 884–96.
- Hübner NS, Mechling AE, Lee H-L, Reisert M, Bienert T, Hennig J, et al. The connectomics of brain demyelination: functional and structural patterns in the cuprizone mouse model. *Neuroimage* 2017; 146: 1–18.
- Jones MW, Wilson MA. Theta rhythms coordinate hippocampal–prefrontal interactions in a spatial memory task. *PLoS Biol* 2005; 3: e402.

- Kochunov P, Thompson PM, Lancaster JL, Bartzokis G, Smith S, Coyle T, et al. Relationship between white matter fractional anisotropy and other indices of cerebral health in normal aging: tract-based spatial statistics study of aging. *Neuroimage* 2007; 35: 478–87.
- Kovács T. Mechanisms of olfactory dysfunction in aging and neurodegenerative disorders. *Ageing Res Rev* 2004; 3: 215–32.
- Kuchibhotla KV, Lattarulo CR, Hyman BT, Bacskai BJ. Synchronous hyperactivity and intercellular calcium waves in astrocytes in Alzheimer mice. *Science* 2009; 323: 1211–5.
- Latif-Hernandez A, Shah D, Craessaerts K, Saido T, Saito T, De Strooper B, et al. Subtle behavioral changes and increased prefrontal-hippocampal network synchronicity in APPNL-G-F mice before prominent plaque deposition. *Behav Brain Res* 2019; 364: 431–41.
- Laurent C, Dorothée G, Hunot S, Martin E, Monnet Y, Duchamp M, et al. Hippocampal T cell infiltration promotes neuroinflammation and cognitive decline in a mouse model of tauopathy. *Brain* 2017; 140: 184–200.
- Lee I, Solivan F. The roles of the medial prefrontal cortex and hippocampus in a spatial paired-association task. *Learn Mem* 2008; 15: 357–67.
- Liu D, Lu H, Stein E, Zhou Z, Yang Y, Mattson MP. Brain regional synchronous activity predicts tauopathy in 3xTgAD mice. *Neurobiol Aging* 2018; 70: 160–9.
- Liu P-P, Xie Y, Meng X-Y, Kang J-S. History and progress of hypotheses and clinical trials for Alzheimer's disease. *Sig Transduct Target Ther* 2019; 4: 1–22.
- Martel G, Simon A, Nocera S, Kalainathan S, Pidoux L, Blum D, et al. Aging, but not tau pathology, impacts olfactory performances and somatostatin systems in THY-Tau22 mice. *Neurobiol Aging* 2015; 36: 1013–28.
- Mechling AE, Hübner NS, Lee H-L, Hennig J, Von Elverfeldt D, Harsan, LA. Fine-grained mapping of mouse brain functional connectivity with resting-state fMRI. *NeuroImage* 2014; 96: 203. doi: 10.1016/j.neuroimage.2014.03.078.
- Miller MI, Younes L, Ratnanather JT, Brown T, Trinh H, Lee DS, et al. Amygdalar atrophy in symptomatic Alzheimer's disease based on diffeomorphometry: the BIOCARD cohort. *Neurobiol Aging* 2015; 36 (Suppl 1): S3–S10.
- Ortner M, Pasquini L, Barat M, Alexopoulos P, Grimmer T, Förster S, et al. Progressively disrupted intrinsic functional connectivity of basolateral amygdala in very early Alzheimer's disease. *Front Neurol* 2016; 7: 132.
- Phelps EA. Human emotion and memory: interactions of the amygdala and hippocampal complex. *Curr Opin Neurobiol* 2004; 14: 198–202.
- Poulin SP, Dautoff R, Morris JC, Barrett LF, Dickerson BC. Alzheimer's disease neuroimaging initiative. Amygdala atrophy is prominent in early Alzheimer's disease and relates to symptom severity. *Psychiatry Res* 2011; 194: 7–13.
- Rajmohan V, Mohandas E. The limbic system. *Indian J Psychiatry* 2007; 49: 132–9.
- Reisert M, Kiselev VG. Fiber continuity: an anisotropic prior for ODF estimation. *IEEE Trans Med Imaging* 2011; 30: 1274–83.
- Ringman JM, O'Neill J, Geschwind D, Medina L, Apostolova LG, Rodriguez Y, et al. Diffusion tensor imaging in preclinical and pre-symptomatic carriers of familial Alzheimer's disease mutations. *Brain J Neurol* 2007; 130: 1767–76.
- Schindowski K, Bretteville A, Leroy K, Bégard S, Brion J-P, Hamdane M, et al. Alzheimer's disease-like tau neuropathology leads to memory deficits and loss of functional synapses in a novel mutated tau transgenic mouse without any motor deficits. *Am J Pathol* 2006; 169: 599–616.
- Schultz SA, Strain JF, Adedokun A, Wang Q, Preische O, Kuhle J, et al. Serum neurofilament light chain levels are associated with white matter integrity in autosomal dominant Alzheimer's disease. *Neurobiology of Disease* 2020; 142: 104960.
- Serrano-Pozo A, Frosch MP, Masliah E, Hyman BT. Neuropathological alterations in Alzheimer disease. *Cold Spring Harb Perspect Med* 2011; 1: a006189.
- Shah D, Praet J, Latif Hernandez A, Höfling C, Anckaerts C, Bard F, et al. Early pathologic amyloid induces hypersynchrony of BOLD resting-state networks in transgenic mice and provides an early therapeutic window before amyloid plaque deposition. *Alzheimers Dement* 2016; 12: 964–76.
- Sheline YI, Raichle ME. Resting state functional connectivity in pre-clinical Alzheimer's disease. *Biol Psychiatry* 2013; 74: 340–7.
- Smith SM, Miller KL, Salimi-Khorshidi G, Webster M, Beckmann CF, Nichols TE, et al. Network modelling methods for FMRI. *Neuroimage* 2011; 54: 875–91.
- Soler H, Dorca-Arévalo J, González M, Rubio SE, Ávila J, Soriano E, et al. The GABAergic septohippocampal connection is impaired in a mouse model of tauopathy. *Neurobiol Aging* 2017; 49: 40–51.
- Sourty M, Thoraval L, Roquet D, Armspach J-P, Foucher J, Blanc F. Identifying dynamic functional connectivity changes in dementia with Lewy bodies based on product hidden Markov models. *Front Comput Neurosci* 2016; 10: 60.
- Stephen JM, Montaña R, Donahue CH, Adair JC, Knoefel J, Qualls C, et al. Somatosensory responses in normal aging, mild cognitive impairment, and Alzheimer's disease. *J Neural Transm Vienna Transm* 2010; 117: 217–25.
- Thomas AG, Koumellis P, Dineen RA. The Fornix in health and disease: an imaging review. *RadioGraphics* 2011; 31: 1107–21.
- Van Cauter T, Camon J, Alvernhe A, Elduayen C, Sargolini F, Save E. Distinct roles of medial and lateral entorhinal cortex in spatial cognition. *Cereb Cortex* 2013; 23: 451–9.
- Van der Jeugd A, Vermaercke B, Derisbourg M, Lo AC, Hamdane M, Blum D, et al. Progressive age-related cognitive decline in tau mice. *J Alzheimers Dis* 2013; 37: 777–88.
- Veraart J, Novikov DS, Christiaens D, Ades-Aron B, Sijbers J, Fieremans E. Denoising of diffusion MRI using random matrix theory. *Neuroimage* 2016; 142: 394–406.
- Wilson RS, Arnold SE, Schneider JA, Boyle PA, Buchman AS, Bennett DA. Olfactory impairment in presymptomatic Alzheimer's disease. *Ann N Y Acad Sci* 2009; 1170: 730–5.
- Wu JW, Hussaini SA, Bastille IM, Rodriguez GA, Mrejeru A, Rilet K, et al. Neuronal activity enhances tau propagation and tau pathology in vivo. *Nat Neurosci* 2016; 19: 1085–92.
- Xie R, Fang M, Zhou L, Fan S, Liu J, Quan H, et al. Diffusion tensor imaging detects Wallerian degeneration of the corticospinal tract early after cerebral infarction. *Neural Regen Res* 2012; 7: 900–5.
- Yao H, Liu Y, Zhou B, Zhang Z, An N, Wang P, et al. Decreased functional connectivity of the amygdala in Alzheimer's disease revealed by resting-state fMRI. *Eur J Radiol* 2013; 82: 1531–8.
- Zhan J, Lin T-H, Libbey JE, Sun P, Ye Z, Song C, et al. Diffusion basis spectrum and diffusion tensor imaging detect hippocampal inflammation and dendritic injury in a virus-induced mouse model of epilepsy. *Front Neurosci* 2018; 12: 77.